

Normal Spectral Emissivity Measurement of Liquid Iron and Nickel Using Electromagnetic Levitation in Direct Current Magnetic Field

HIDEKAZU KOBATAKE, HOSSEIN KHOSROABADI, and HIROYUKI FUKUYAMA

Normal spectral emissivities of liquid iron and nickel were measured for wavelengths of 780 to 920 nm by direct measurement of normal spectral radiance using electromagnetic levitation in a direct current (DC) magnetic field. A DC magnetic field suppressed surface oscillation and the transitional motion of the liquid metal droplets. The normal spectral emissivities of both liquid iron and nickel show weak negative wavelength dependence and have negligible temperature dependence. The normal spectral emissivities of liquid iron and nickel at 807 nm were determined respectively as 0.394 ± 0.012 (1600 K to 1950 K (1327 °C to 1677 °C)) and 0.368 ± 0.004 (1720 K to 1825 K (1447 °C to 1552 °C)). The experimental uncertainty used here is double the value of the standard deviation.

DOI: 10.1007/s11661-012-1101-0

© The Minerals, Metals & Materials Society and ASM International 2012

I. INTRODUCTION

NUMERICAL simulations have been developed to improve casting and welding processes of Fe-based alloys and Ni-based superalloys, which are widely used in automobile, aerospace, and power generation industries. Accurate thermophysical properties of these alloys are necessary for precise simulation. To meet those needs, we developed noncontact laser modulation calorimetry using electromagnetic levitation in a direct current (DC) magnetic field, which enables accurate measurements of heat capacity, hemispherical total emissivity, and thermal conductivity of high-temperature liquid metals.^[1–6] Transitional motion, surface oscillation of a droplet, and convection in a droplet were suppressed efficiently by superimposing a DC magnetic field on a levitating droplet. For this technique, normal spectral emissivity at a heating laser wavelength (807 nm) is necessary to estimate the laser absorptivity for heat capacity measurements. Therefore, we must also develop normal spectral emissivity measurements of liquid metals. In 2005, the normal spectral emissivity of liquid silicon was measured using the experimental uncertainty of 5 pct with electromagnetic levitation.^[7] The uncertainty in this measurement using an electromagnetic levitation is caused by surface oscillation or by translational motion of the levitated liquid silicon. To reduce the uncertainty further, a DC magnetic field was applied to the levitated liquid silicon. Good results were obtained because of the suppressed fluctuations of temperature and radiance during the emissivity mea-

surements.^[8] The normal spectral emissivities of liquid iron and nickel were measured in this study using the technique of that earlier study. The applicability of the Drude free electron model and experimental uncertainty were discussed based on those results.

II. EXPERIMENTAL

A. Principle

The definition of the normal spectral emissivity of a sample, $\varepsilon_s(\lambda, T)$, is the ratio of the normal spectral radiance emitted from a sample $R_s(\lambda, T)$ to that from a blackbody $R_b(\lambda, T)$ at the same wavelength λ and temperature T , as shown subsequently.

$$\varepsilon(\lambda, T) = \frac{R_s(\lambda, T)}{R_b(\lambda, T)} \quad [1]$$

The value of $R_b(\lambda, T)$ is calculable using Planck's law of radiation, which is expressed as the following equation:

$$R_b = \frac{C_1}{\lambda^5 [\exp(C_2/\lambda T) - 1]} \quad [2]$$

In that equation, $C_1 = 3.742 \times 10^{-16}$ (W m²) and $C_2 = 1.439 \times 10^{-2}$ (m K) are constants. Therefore, normal spectral emissivity can be determined through experimental measurement of the spectral radiance of the sample as a function of wavelength and temperature. In this study, the radiances emitted from an electromagnetically levitated liquid nickel or iron in a DC magnetic field were measured using a calibrated spectrometer.

B. Calibration of the Spectrometer

A multichannel spectrometer (USB2000; Ocean Optics Inc., FL) with a grating monochromator covering

HIDEKAZU KOBATAKE, Assistant Professor, HOSSEIN KHOSROABADI, Postdoctor, and HIROYUKI FUKUYAMA, Professor, are with the Institute of Multidisciplinary Research for Advanced Materials, Tohoku University, Miyagi, Sendai 980-8577, Japan. Contact e-mail: fukuyama@tagen.tohoku.ac.jp

Manuscript submitted August 1, 2011.

Article published online March 28, 2012

wavelengths of 530 to 1100 nm and optical resolution of 4.0 nm was used for radiance measurements. A quasi-blackbody made of graphite was used as a standard light source for spectrometer calibration. The quasi-blackbody has two cavities located, respectively, at the top and bottom. Each cavity was 5 mm in diameter and 35-mm deep, providing emissivity greater than 0.998.^[9] Each cavity was surrounded by a copper metal bath to achieve the homogenized temperature distribution in the quasi-blackbody. The top cavity was used for calibration of the spectrometer, whereas the bottom one was used for temperature measurements of the quasi-blackbody using a single-color-optical pyrometer (1350-nm measurement wavelength with 1100- to 1500-nm bandwidth, IR-CAQ2CS; Chino Corp., Tokyo). The pyrometer was calibrated using a plateau temperature that can be detected during the melting or solidification process of copper in the surrounding metal bath. The detailed design of the quasi-blackbody was described in an earlier report.^[8]

C. Experimental Setup

Figure 1 depicts the experimental apparatus that is used for spectral emissivity measurements. The optical system comprises a window, a collective lens, a beam splitter, and a glass fiber attached to a spectrometer. A diaphragm (2-mm diameter, 50-mm length) was placed 750 mm above the quasi-blackbody or levitated liquid metals to obtain their normal radiance. The quasi-blackbody, supported by a 10-mm-diameter quartz glass tube, was placed at the same position at which the liquid metals were levitated. The quasi-blackbody was heated

uniformly using a solenoid coil. The levitation coil for liquid metals consists of two parts. The upper part is a solenoid coil with two turns for stabilization of the levitated liquid. The lower part is a solenoid coil with five turns for lifting up the liquid metals. The coils were connected to a high-frequency power source (150 to 450 kHz frequency range, 10 kW maximum power, Easy Heat 8310; Ameritherm Inc., New York, NY). A superconducting magnet with a 120-nm bore (TD-10T120SSF; Japan Superconductor Technology Inc., Kobe) was used to apply a DC magnetic field.

D. Experimental Procedure

A iron or nickel sample (sample mass: 1.30 to 1.50 g, purities of nickel and iron were 99 and 99.5 pct, respectively; Nilaco Corp., Tokyo) was placed at the center of the levitation coil. After the sample setup, the chamber was evacuated using a rotary pump in combination with a turbo molecular pump to obtain a vacuum level of 10^{-2} Pa. The chamber was purged with Ar-5 vol pct H_2 gas to prevent oxidation of the sample. Liquid iron and nickel were levitated electromagnetically in an Ar-5 vol pct H_2 gas flow atmosphere. In addition, He gas was introduced to the chamber as a cooling gas to control the liquid metal temperature. Using a superconducting magnet, a DC magnetic field of 5 T was imposed to suppress surface oscillation and translational motion.

The normal spectral radiation from the liquid metal was measured using the spectrometer through the same optical path as that used for the spectrometer calibration. The center of the optical alignment was adjusted to the center of the sample or the quasi-blackbody using a CCD camera attached to the optical system. The sample temperature was measured using the pyrometer and was calibrated based on Planck's law using the melting point, assuming that the normal spectral emissivity of the sample at the pyrometer wavelength is constant.

III. RESULTS

A. Calibration of the Spectrometer

Figure 2 presents a typical temperature profile of the quasi-blackbody during heating and cooling processes. The average temperatures with their standard deviation at two plateaus were 1357.5 ± 0.9 K and 1357.5 ± 0.7 K, respectively, during the melting and solidification process. The pyrometer was calibrated at this temperature.

Figure 3 portrays the relation between spectral radiance and the output count intensity of the spectrometer obtained from the spectral radiance emitted from the quasi-blackbody at 800- and 900-nm wavelengths. The spectral radiances are given by Planck's law at the corresponding temperature and wavelength. A good linear relation was confirmed between spectral radiance and the output count intensity. Using this relation, the sample radiance at a given temperature and wavelength was determined.

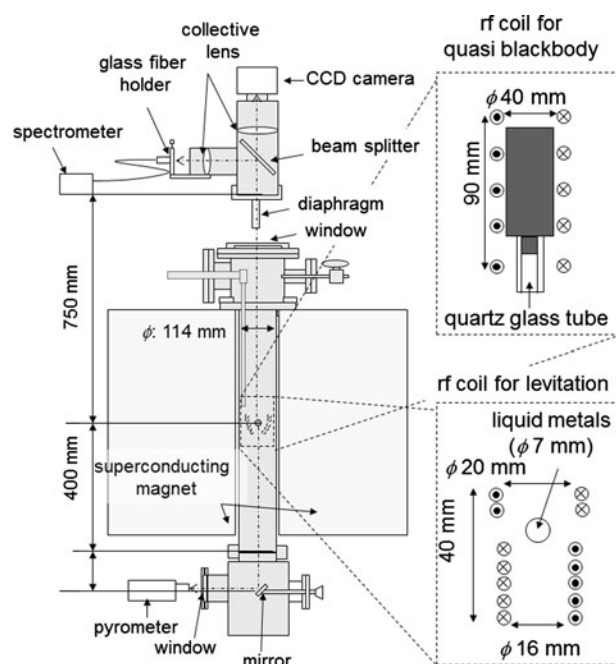


Fig. 1—Schematic illustration of the experimental facility. Coil designs for levitation and for heating of the quasi-blackbody are also shown.

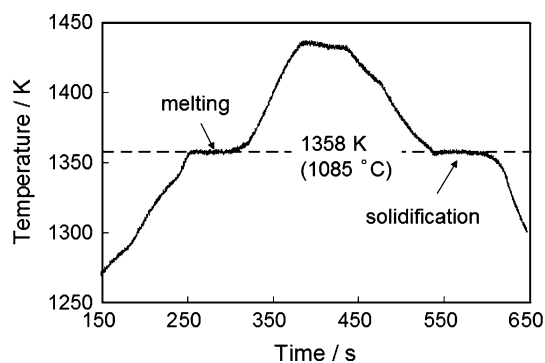


Fig. 2—Temperature profile of the quasi-blackbody during melting and solidification of Cu in the metal bath. The quasi-blackbody temperature was calibrated using the plateau detected at the melting and solidification point of Cu.

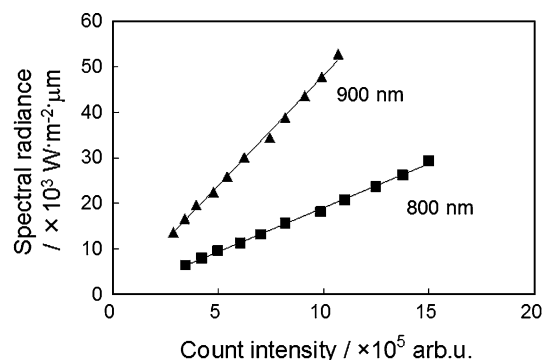


Fig. 3—Relation between spectral radiance and output count intensity of the spectrometers: square at 800 nm and triangle at 900 nm.

B. Temperature Profile of Liquid Iron

Figure 4 presents temperature profiles during the spectral radiance measurement of liquid iron. After complete melting of the iron sample, the temperature was adjusted by controlling the He gas flow rate in the chamber. A sudden temperature increase observed at around 1650 seconds resulted from the recalescence process because of the liquid iron solidification. A similar temperature profile was obtained also during the spectral radiance measurement of liquid nickel.

C. Normal Spectral Emissivity of Liquid Iron

Figure 5(a) portrays the wavelength dependence of the normal spectral emissivity of liquid iron at 1819 K (1546 °C). The normal spectral emissivity of liquid iron shows negative wavelength dependence. It decreases between 780 to 920 nm from 0.40 at 780 nm to 0.36 at 920 nm. Data measured at 1890 K (1617 °C) using an ellipsometer in an earlier study^[10] are shown in the figure, revealing similar wavelength dependence.

Figure 5(b) shows the temperature dependence of normal spectral emissivity of liquid iron at 807 and 900 nm with data from the literature obtained at 807 nm.^[10,11] Further, the literature data at 684.5 nm measured by the pulse heating technique combined with fast ellipsometry^[12,13] are also plotted. The temperature

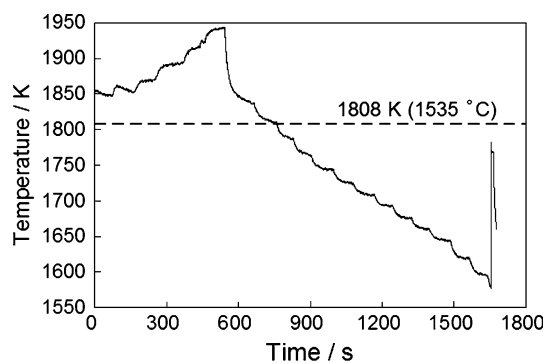


Fig. 4—Temperature profile of liquid iron during normal spectral emissivity measurement.

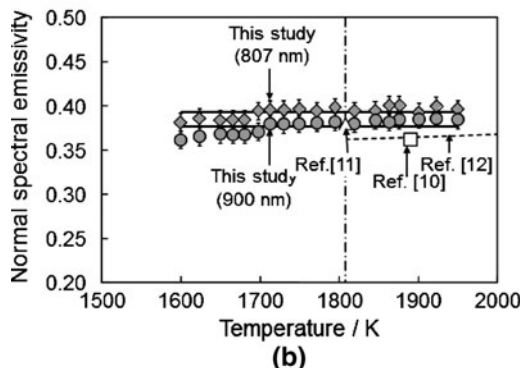
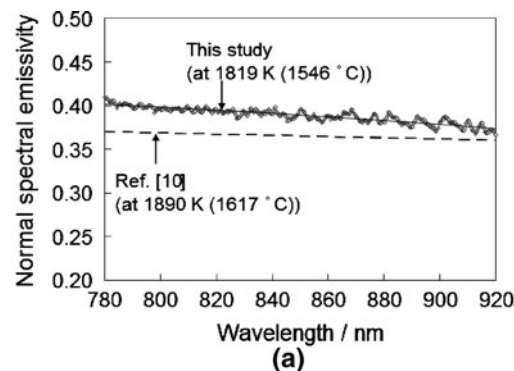


Fig. 5—(a) Wavelength dependence of normal spectral emissivity for liquid iron at 1819 K (1546 °C) with literature data (dashed line)^[10] and (b) temperature dependence of normal spectral emissivity at 807 nm (◇) and at 900 nm (○) with literature data (□^[10] and △^[11] at 807 nm and dashed line^[12] at 684.5 nm).

dependence of the emissivity measured in this study is negligible, and the average value of the emissivity at 807 nm is determined as 0.394 ± 0.012 at temperatures of 1600 K to 1950 K (1327 °C to 1677 °C). The experimental uncertainty used here is double the value of the standard deviation. The normal spectral emissivity measured in this study shows good agreement with the value, as measured using the cold crucible method.^[11] The similar negligible temperature dependence of the emissivity was obtained for the entire wavelength range measured in this study. This fact supports the validation of the temperature measurements using the pyrometer.

D. Normal Spectral Emissivity of Liquid Nickel

Figure 6(a) shows the wavelength dependence of normal spectral emissivity of liquid nickel at 1726 K (1453 °C). The emissivity shows negative wavelength dependence and decreases from 0.38 to 0.34. Data obtained in an earlier study, measured at 1764 K (1491 °C) using an ellipsometer,^[10] are also shown in the figure, showing good agreement with the results obtained in the present study.

Figure 6(b) shows the temperature dependence of normal spectral emissivity of liquid nickel at 807 and 900 nm with data from the literature obtained at 807 nm.^[10,11,14] Further, the literature data at 684.5 nm measured by the pulse heating technique combined with fast ellipsometry^[12,13] are also plotted. The temperature dependence of the emissivity measured in this study is negligible, and the average value of the emissivity at 807 nm is determined as 0.368 ± 0.004 at temperatures of 1720 K to 1825 K (1447 °C to 1552 °C). The experimental uncertainty is double that of the standard deviation. This value is consistent, within uncertainty, with data reported in the literature.^[10] The temperature dependence of the emissivity was negligible for the entire wavelength range measured in this study, which validates the temperature measurement using the pyrometer.

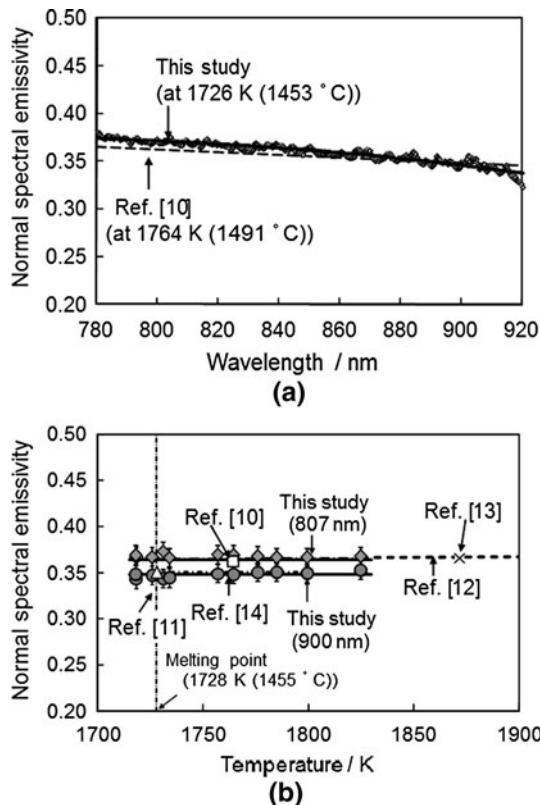


Fig. 6—(a) Wavelength dependence of normal spectral emissivity for liquid nickel at 1726 K (1453 °C) with literature data (dashed line)^[10] and (b) temperature dependence of normal spectral emissivity at 807 nm (◇) and at 900 nm (○) with literature data (□,^[10] △^[11] and dashed-dotted line^[14] at 807 nm and ×^[13] and dashed line^[12] at 684.5 nm).

IV. DISCUSSION

A. Applicability of the Drude Model

The simple Drude model reproduced the wavelength dependence of the emissivity of liquid silicon.^[7,8] In this study, the Drude model was also applied to explain the wavelength dependence of the normal spectral emissivities of liquid iron and nickel.

Emissivity of opaque material in a thermal equilibrium is expressed using the refractive index n and extinction coefficient k as

$$\varepsilon = \frac{4n}{(n+1)^2 + k^2} \quad [3]$$

These optical constants are given using the real and imaginary parts $\varepsilon_1(\omega)$ and $\varepsilon_2(\omega)$ of the dielectric function as

$$n^2 - k^2 = \varepsilon_1(\omega) = 1 - \frac{\omega_p^2 \tau^2}{1 + \omega^2 \tau^2} \quad [4]$$

and

$$2nk = \varepsilon_2(\omega) = \frac{\omega_p^2 \tau}{\omega(1 + \omega^2 \tau^2)} \quad [5]$$

where ω denotes the angular frequency of the electric field, τ represents the relaxation time, and ω_p is the plasma frequency, which is calculated as

$$\omega_p^2 = \frac{Ne^2}{m\varepsilon_0} \quad [6]$$

where N is the number of free electrons per unit volume, m represents the effective mass of electron, e is the electron charge, and ε_0 is the permittivity of vacuum. The values of N for liquid iron and nickel are calculated using their densities.^[15] The relaxation times τ of those liquids are determined from the electrical resistivities ρ_{el} ^[16] using the following equation:

$$\tau = \frac{m}{\rho_{el} Ne^2} \quad [7]$$

Figure 7 presents a comparison of the present experimentally obtained results with calculated values using the Drude model for (a) iron and (b) nickel at their melting points. Table I presents the parameters used for the estimation of the normal spectral emissivity of liquid iron and nickel. The experimental values of liquid iron are well reproducible with the Drude model, as portrayed in Figure 7(a). As shown in Figure 7(b), the experimental values of liquid nickel deviate slightly from the Drude model. Because electrical resistivity strongly affects the calculated value using the Drude model, this deviation might be explained by the uncertainty in electrical resistivity.

The previous studies^[12,13] suggested that the normal spectral emissivity at 684.5 nm measured using the ellipsometry cannot be well explained by the simple Drude model. The Drude model is only applicable for the longer wavelength region, where the intraband transition of the free electron dominantly contributes the radiation property. Therefore, the difference

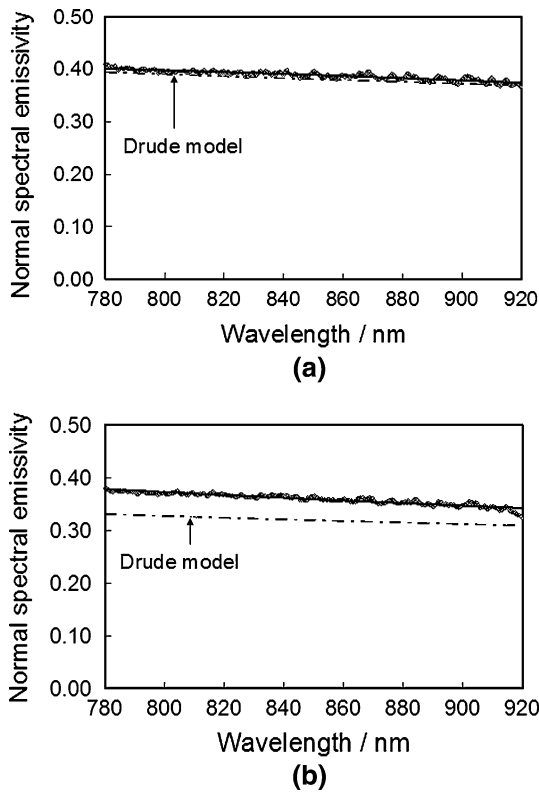


Fig. 7—Comparison of wavelength dependence of normal spectral emissivity in this study and values calculated using the Drude model (dashed line) for (a) liquid iron and (b) liquid nickel.

Table I. Parameters Used for Calculation of Normal Spectral Emissivity of Liquid Iron and Nickel Using the Drude Model at Their Melting Temperatures

Parameters	Liquid Iron at 1808 K (1535 °C)	Liquid Nickel at 1728 K (1455 °C)
$\rho/\text{kg m}^{-3}$ ^[15]	7.037×10^3	7.849×10^3
$\rho_{el}/\Omega \text{ m}$ ^[16]	1.46×10^{-6}	0.93×10^{-6}
N/m^{-3}	1.44×10^{32}	1.61×10^{32}
$\omega_p/\text{rad s}^{-1}$	6.78×10^{17}	7.16×10^{17}
τ/s	1.69×10^{-19}	2.36×10^{-19}
m/kg	9.109×10^{-31}	
e/C	1.602×10^{-19}	
$\epsilon_0/\text{F m}^{-1}$	8.854×10^{-12}	
Avogadro's constant/ mol^{-1}	6.022×10^{23}	

between the Drude model and the previous studies^[12,13] may be caused by the effect of the interband transition of electron. The effect of the interband transition cannot be detected in the present study at a wavelength range from 780 to 920 nm.

In the cases of solid iron and nickel, the Drude–Roberts model reproduced the normal spectral emissivities of solid iron and nickel,^[14,17–19] which consist of contributions of the interband and intraband transitions of electrons. The intraband term includes more than one class of conduction electrons having different relaxation times, because the Fermi levels are in the region of the overlap of the 3d-electron band and the 4s-electron band.^[20]

In the cases of liquid iron and nickel, the simple Drude model is apparently sufficient to reproduce the present experimentally obtained results. Fujiwara^[21] investigated the density of state of 3d electrons in liquid iron and nickel using molecular dynamics. The centers of d-band energies of liquid iron and nickel are, respectively, smaller by 18 and 24 pct with respect to the Fermi energies. Therefore, the effect of the 3d band electron is negligible in the liquids.

B. Validity of Pyrometer Calibration

We calibrated the optical pyrometer at melting points of iron and nickel, and assumed that the normal spectral emissivities at 1350 nm used for the pyrometer are constant in the experimental temperature range. This assumption was examined using the Drude model as follows. The temperature dependence of the infrared region of liquid iron and nickel can be estimated from the temperature dependence of their density and the electrical resistivity using the Drude model. From this calculation, the normal spectral emissivities present weak positive temperature dependences. In the experimental temperature range, the normal spectral emissivities at 1350 nm would change by 2 pct, which is considered for uncertainty in the emissivity measurements in Section IV–C.

C. Uncertainty of Normal Spectral Emissivities

Uncertainty in normal spectral emissivity measurements mainly comprises the following components: (1) uncertainty of the radiance measurements obtained using the spectrometer, (2) uncertainty in temperature measurements, and (3) uncertainty in the spectrometer wavelength. The combined standard uncertainty in emissivity $\sigma(\epsilon)$ is given as the following equation:

$$\{\sigma(\epsilon)\}^2 = \left\{ \frac{\partial \epsilon}{\partial R_s} \sigma(R_s) \right\}^2 + \left\{ \frac{\partial \epsilon}{\partial T} \sigma(T_{\text{fluctuation}}) \right\}^2 + \left\{ \frac{\partial \epsilon}{\partial T} \sigma(T_{\text{emissivity}}) \right\}^2 + \left\{ \frac{\partial \epsilon}{\partial \lambda} \sigma(\lambda) \right\}^2 \quad [8]$$

The contributions of each component to the uncertainties for liquid iron and for liquid nickel are summarized, respectively, in Tables II and III according to the “guide to uncertainty in measurement” (GUM).^[22] The temperature uncertainty was attributed to the fluctuation of temperature, $T_{\text{fluctuation}}$, and to the uncertainty in the calibrated emissivity at 1350 nm, $T_{\text{emissivity}}$, and to the bandwidth, $T_{\text{bandwidth}}$, used for the pyrometer. The former, $T_{\text{fluctuation}}$, is estimated as 0.6 K from the standard deviation of temperature during emissivity measurements. However, $T_{\text{emissivity}}$ is estimated as 4 K from the temperature dependence of the normal spectral emissivity, as explained in Section IV–B. The uncertainty in temperature measurement caused by the pyrometer bandwidth (1100 to 1500 nm) was estimated using the shortest and longest wavelengths. The liquid iron temperature of 1950.00 K (1677 °C) measured at 1350 nm would vary from 1950.14 K to 1949.89 K (1676.99 °C to 1476.74 °C) considering the bandwidth.

Table II. Uncertainty in Normal Spectral Emissivity of Liquid Iron

Component	Standard Uncertainty	Sensitivity Coefficient	Contribution
$R_s(\lambda, T)$	49 W m ⁻² μm	$\partial \varepsilon / \partial R_s(\lambda, T) = 1.65 \times 10^{-5} / \text{W}^{-1} \text{ m}^2 \mu\text{m}^{-1}$	0.0004
$T_{\text{fluctuation}}$	0.6 K	$\partial \varepsilon / \partial T_{\text{fluctuation}} = 2.61 \times 10^{-4} / \text{K}^{-1}$	0.0011
$T_{\text{emissivity}}$	4.0 K	$\partial \varepsilon / \partial T_{\text{emissivity}} = 2.61 \times 10^{-4} / \text{K}^{-1}$	0.0079
λ	2 nm	$\partial \varepsilon / \partial \lambda = -0.118 \times 10^{-3} \text{ nm}^{-1}$	-0.0022
Combined uncertainty			0.008
Expanded uncertainty (coverage factor = 2)			0.016
$T = 1950 \text{ K}$, $\varepsilon_s = 0.397$, and $\lambda = 807 \text{ nm}$.			

Table III. Uncertainty in Normal Spectral Emissivity of Liquid Nickel

Component	Standard Uncertainty	Sensitivity Coefficient	Contribution
$R_s(\lambda, T)$	49 W m ⁻² μm	$\partial \varepsilon / \partial R_s(\lambda, T) = 1.65 \times 10^{-5} / \text{W}^{-1} \text{ m}^2 \mu\text{m}^{-1}$	0.0008
$T_{\text{fluctuation}}$	0.6 K	$\partial \varepsilon / \partial T_{\text{fluctuation}} = 2.61 \times 10^{-4} / \text{K}^{-1}$	0.0011
$T_{\text{emissivity}}$	4.0 K	$\partial \varepsilon / \partial T_{\text{emissivity}} = 2.61 \times 10^{-4} / \text{K}^{-1}$	0.0076
λ	2 nm	$\partial \varepsilon / \partial \lambda = -0.118 \times 10^{-3} \text{ nm}^{-1}$	-0.0022
Combined uncertainty			0.008
Expanded uncertainty (coverage factor = 2)			0.016
$T = 1825 \text{ K}$, $\varepsilon_s = 0.356$, and $\lambda = 807 \text{ nm}$.			

This variation is much smaller than the temperature fluctuation. Therefore, the effect of pyrometer bandwidth was omitted from the uncertainty evaluation. The spectrometer has a wavelength resolution of 4 nm, which implies uncertainty of 2 nm in the obtained wavelength value. The combined standard uncertainties are evaluated as 0.008 for both liquid iron and nickel. Therefore, the expanded uncertainty at the 95.45 pct level of confidence (coverage factor = 2) was 0.016, as presented in Tables II and III.

V. CONCLUSIONS

Normal spectral emissivities of liquid iron and nickel were measured for wavelengths of 780 to 920 nm using the electromagnetic levitator in a DC magnetic field. The emissivities exhibit a weak negative wavelength dependence and negligible temperature dependence. The measured normal spectral emissivity values at 807 nm are summarized with double the standard deviation, as shown subsequently.

Liquid iron : $\varepsilon_s = 0.394 \pm 0.012$ (1600 K to 1950 K
(1327°C to 1677°C))

Liquid nickel : $\varepsilon_s = 0.368 \pm 0.004$ (1720 K to 1825 K
(1447°C to 1552°C))

The experimental uncertainty used here is double the value of the standard deviation. The experimental values are well reproducible with the Drude model within reasonable experimental uncertainty, which indicates that the thermal radiation is controlled mainly by the transfer of free electrons in the liquids.

ACKNOWLEDGMENT

This work was financially supported by SENTAN, Japan Science and Technology Agency (JST).

REFERENCES

1. H. Fukuyama, H. Kobatake, K. Takahashi, I. Minato, T. Tsukada, and S. Awaji: *Meas. Sci. Technol.*, 2007, vol. 18, p. 2059.
2. H. Kobatake, H. Fukuyama, I. Minato, T. Tsukada, and S. Awaji: *Appl. Phys. Lett.*, 2007, vol. 90, p. 094102.
3. T. Tsukada, H. Fukuyama, and H. Kobatake: *Int. J. Heat Mass Transfer*, 2007, vol. 50, pp. 3054–61.
4. H. Kobatake, H. Fukuyama, I. Minato, T. Tsukada, and S. Awaji: *J. Appl. Phys.*, 2008, vol. 104, p. 054901.
5. H. Fukuyama, K. Takahashi, S. Sakashita, H. Kobatake, T. Tsukada, and S. Awaji: *ISIJ Int.*, 2009, vol. 49, pp. 1436–42.
6. H. Kobatake, H. Fukuyama, T. Tsukada, and S. Awaji: *Meas. Sci. Technol.*, 2010, vol. 21, p. 025901.
7. H. Kawamura, H. Fukuyama, M. Watanabe, and T. Hibiya: *Meas. Sci. Technol.*, 2005, vol. 16, pp. 386–93.
8. H. Kobatake, H. Khosroabadi, and H. Fukuyama: *Meas. Sci. Technol.*, 2011, vol. 22, p. 015102.
9. De Vos J: *C. Physica*, 1954, vol. 20, pp. 669–89.
10. S. Krishnan, K. Yugawa, and P. C. Nordine: *Phys. Rev. B*, 1997, vol. 55, pp. 8201–06.
11. H. Watanabe, M. Susa, H. Fukuyama, and K. Nagata: *Int. J. Thermo.*, 2003, vol. 24, pp. 473–88.
12. B. Wilthan, C. Cagran, G. Pottlacher, and E. Kaschnitz: *Monatshefte Chemie*, 2005, vol. 136, pp. 1971–76.
13. C. Cagran, B. Wilthan, and G. Pottlacher: *High Temp. High Press.*, 2003–2007, vol. 35–36, pp. 667–75.
14. T. Makino: *Int. J. Thermophys.*, 1990, vol. 11, pp. 339–52.
15. T. Nishizuka, Y. Sato, T. Takamizawa, K. Sugisawa, and T. Yamamura: *Proc. 16th Eur. Conf. on Thermophysical Properties*, Imperial College, London, 2002.
16. R.S. Hixson, M.A. Winkler, and M.L. Hodgdon: *Phys. Rev. B*, 1990, vol. 42, pp. 6485–91.
17. S. Roberts: *Phys. Rev.*, 1959, vol. 114, pp. 104–15.
18. T. Makino and T. Kunitomo: *Bull. JSME*, 1977, vol. 20, pp. 1607–14.
19. T. Makino, T. Kawasaki, and T. Kunitomo: *Bull. JSME*, 1982, vol. 25, pp. 804–11.

20. L.F. Mattheiss: *Phys. Rev.*, 1964, vol. 134, pp. A970–A973.
21. T. Fujiwara: *J. Phys. F: Met. Phys.*, 1979, vol. 9, pp. 2011–24.
22. L. Kirkup and R.B. Frenkel: *An Introduction to Uncertainty in Measurement*, Cambridge University Press, Cambridge, United Kingdom, 2006, pp. 35–52.